Pergamon

SCIENCE DIRECT®

Tetrahedron 59 (2003) 10485–10497

TETRAHEDRON

Catalytic asymmetric epoxidation of α,β-unsaturated carboxylic acid imidazolides and amides by lanthanide–BINOL complexes

Takashi Ohshima, Tetsuhiro Nemoto, Shin-ya Tosaki, Hiroyuki Kakei, Vijay Gnanadesikan and Masakatsu Shibasaki*

Graduate School of Pharmaceutical Sciences, The University of Tokyo, Hongo, Bunkyo-ku, Tokyo 113-0033, Japan

Received 2 May 2003; accepted 4 June 2003

Abstract—Highly enantioselective catalytic asymmetric epoxidation of α,β-unsaturated carboxylic acid imidazolides and simple amides was developed. In the presence of 5–10 mol% of lanthanide–BINOL complexes, the reaction proceeded smoothly with high substrate generality. In particular, in the cases of α,β-unsaturated amides, there was nearly perfect enantioselectivity (>99% ee). The corresponding epoxides were successfully transformed into many types of useful chiral compounds such as α,β-epoxy esters, α,β-epoxy amides, α,β-epoxy aldehydes, α,β-epoxy β-keto ester, and α- and β-hydroxy carbonyl compounds. B3LYP density functional studies were performed to predict substrate reactivity.

1. Introduction

Asymmetric epoxidation of α,β-unsaturated carbonyl compounds has attracted a great deal of attention from synthetic organic chemists[1] because it constructs two adjacent chiral carbon centers simultaneously and the corresponding enantiomerically-enriched epoxy compounds can be easily converted to many types of useful chiral compounds.[2] Since the initial report by Juliá and co-workers,[3] catalytic asymmetric epoxidation of α,β-unsaturated ketones (enones) has been studied and several successful methods have been reported.[1,4,5] There are only a few reports, however, of α,β-unsaturated carboxylic acid derivatives. A salen-manganese complex[6] or an optically-active ketone[7] was used for catalytic asymmetric epoxidation of α,β-unsaturated esters. Substrates that have other functional groups, such as a C–C double bond or ketone, cannot be used for those asymmetric reactions due to poor chemoselectivity. Our strategy relies on the Weitz–Scheffer type epoxidation[8] using 1,4-addition of hydroperoxide as an initial step, thus chemoselective epoxidation of electron-deficient alkenes in the presence of other olefins is realized. We recently reported the first example of catalytic epoxidation of α,β-unsaturated carboxylic acid imidazolides by the La–BINOL–$Ph_3As{=}O$ (1:1:1) complex **1** and efficient transformations of the corresponding epoxidation products: α,β-epoxy peroxy *tert*-butyl esters into the α,β-epoxy esters, α,β-epoxy amides, α,β-epoxy aldehydes, and γ,δ-epoxy β-keto esters.[9] We later succeeded in catalytic asymmetric epoxidation of simple α,β-unsaturated amide for the first time.[10] This report details our full investigation of lanthanide–BINOL complex-catalyzed asymmetric epoxidation of α,β-unsaturated carboxylic acid derivatives.

2. Results and discussion

2.1. Catalytic asymmetric epoxidation of α,β-unsaturated carboxylic acid imidazolides

We first examined catalytic asymmetric epoxidation of α,β-unsaturated ester: ethyl (*E*)-cinnamate (**2a**). We previously developed a general and practical catalytic asymmetric epoxidation of α,β-unsaturated ketones using the La–BINOL–$Ph_3As{=}O$ complex **1** generated from $La(O\text{-}i\text{-}Pr)_3$, BINOL, and $Ph_3As{=}O$ in a ratio of 1:1:1.[3d] Using 20 mol% of complex **1**, the epoxidation of **2a** proceeded to afford α,β-epoxy ester **3a** in 90% ee. The obtained yield, however, was only 5% even after 48 h (Scheme 1). To enhance substrate reactivity, we examined

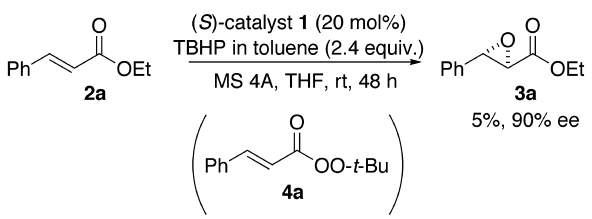

Scheme 1. Catalytic asymmetric epoxidation of ethyl (*E*)-cinnamate (**2a**).

Keywords: asymmetric catalysis; epoxidation; lanthanide; molecular orbital calculation.

* Corresponding author. Tel.: +81-3-5684-0651; fax: +81-3-5684-5206; e-mail: mshibasa@mol.f.u-tokyo.ac.jp

0040–4020/$ - see front matter © 2003 Elsevier Ltd. All rights reserved.
doi:10.1016/j.tet.2003.06.010

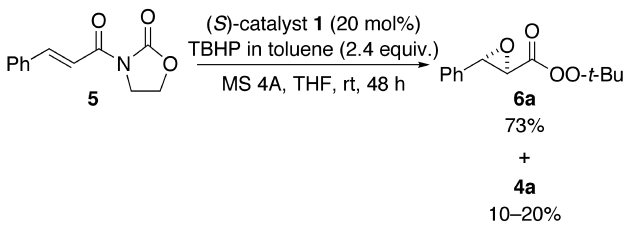

Scheme 2. Catalytic asymmetric epoxidation of *N*-cinnamoyloxazolidinone (**5**).

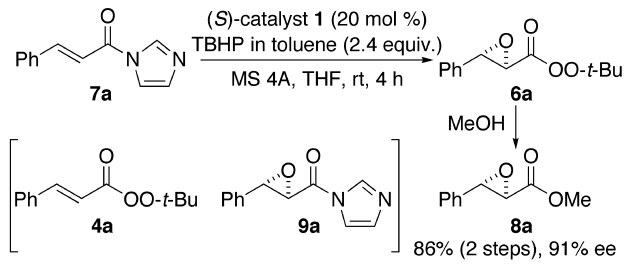

Scheme 3. Catalytic asymmetric epoxidation of *N*-cinnamoylimidazole (**7a**).

more reactive α,β-unsaturated esters, such as *p*-nitrophenyl ester **2b**, pentafluorophenyl ester **2c**, and hexafluoroisopropyl ester **2d** as substrates. In these cases, only transesterification occurred to afford **4a**, which remained unchanged in the reaction medium.

We then turned our attention to catalytic asymmetric epoxidation of activated α,β-unsaturated amides, which would be expected to enhance the reactivity by decreasing the lowest unoccupied molecular orbital (LUMO) energy. *N*-Acyloxazolidinones are one of the most well-known activated amides and they are utilized in various catalytic asymmetric reactions.[11] Thus, we first examined a catalytic asymmetric epoxidation of *N*-cinnamoyloxazolidinone (**5**) using 20 mol% of complex **1**. In contrast to the cases of α,β-unsaturated esters, the reaction proceeded to completion in 48 h, providing an unexpected product: α,β-epoxy peroxycarboxylic acid *tert*-butyl ester **6a** with 10–20% of **4a** (Scheme 2).

To further improve reactivity and selectivity, we investigated other activated α,β-unsaturated amides as substrates. Semiempirical molecular orbital calculation (AM1)[12] revealed that the energy of the LUMO of **5** was 0.216 eV (5.0 kcal/mol) lower than that of **2a**. This result prompted us to perform detailed calculations to find a more reactive substrate. On the basis of our preliminary AM1 calculations, *N*-acylimidazoles (α,β-unsaturated carboxylic acid imidazolide) **7a** was predicted to be a more reactive candidate due to a lower LUMO energy than that of **5**. Later, more precise calculation studies were performed[13] by means of the B3LYP[14] hybrid density functional method using a 6-31G(d) basis set (vide infra). Carboxylic acid imidazolides are widely used in organic synthesis, mainly as acylation reagents.[15] They have not yet been used, however, in an

Table 1. Catalytic asymmetric epoxidation of various cinnamates and the results of AM1 and B3LYP calculations

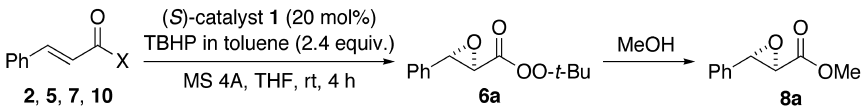

Entry	X	Substrates	LUMO energy (eV)		Time (h)	Yield (%)	ee (%)
			AMI	B3LYP			
1	–OEt	**2a**	−0.68	−1.70	48	5	90
2	$-OC_6F_5$	**2c**		−2.19			
3	–OO-*t*-Bu	**4a**	−0.86	−1.82			
4	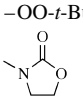	**5**	−0.87	−2.05	24	73	87
5		**7a**	−0.97	−2.34	4	86	91
6		**7b**	−0.99	−2.25	12	70	77
7		**7c**	−1.02	−2.27	3	85	92
8		**7d**	−0.97	−2.34	12	69	87
9		**7e**	−1.07	−2.37	1	91	94
10		**7f**	−0.96	−2.24	24	80	63
11		**10**	−1.07	−2.41	1	Trace	–

asymmetric reaction as a substrate, perhaps because of their high reactivity at the carbonyl carbon toward nucleophiles. Despite these negative factors, we assumed that a soft nucleophile might attack at the β-carbon in preference to the carbonyl carbon. Thus, we investigated a catalytic asymmetric epoxidation using **7a** as a representative starting material. The epoxidation of **7a** proceeded successfully by using the La–BINOL–$Ph_3As{=}O$ complex **1** (20 mol%, rt, 4 h) to afford **8a** in 86% yield with 91% ee with **4a** (5–10%) after direct methanolysis (Scheme 3). During the epoxidation, α,β-epoxy carboxylic acid imidazolide **9a** was not detected by thin-layer chromatography and electronspray ionization-mass analysis. In addition, α,β-unsaturated peroxy ester **4a** was not converted to **6a** under the same conditions. These findings suggest that the epoxidation of **7a** proceeded in preference to transesterification to afford **9a**, which was spontaneously converted to **6a**.

We then investigated the effects of amide moieties in the reaction, which are summarized in Table 1 with the results of AM1 and B3LYP calculations. Among them, 4-phenylimidazolide **7e**, which has a lower LUMO energy than other imidazolides, gave the best result in terms of reactivity, chemical yield, and enantiomeric excess (1 h, 91% yield, 94% ee). In this case, only a trace amount of **4a** was obtained. These results indicated that 4-phenylimidazolide effectively enhanced the reactivity at the β-carbon toward the soft nucleophile. Enhancement of the reactivity appeared to be related to the decrease in LUMO energy with some exception such as triazolide **10**, which afforded the peroxy ester **4a** as a major product.

Having developed an efficient catalytic asymmetric synthesis of **8a** from **7e**, we examined the scope and limitations of different substrates. This newly-developed system had broad generality for epoxidations of various α,β-unsaturated carboxylic acid 4-phenylimidazolides to afford the corresponding epoxides **8a**, **8g–p** (Table 2). When 10 mol% of complex **1** and 2.4 equiv. of *tert*-butyl hydroperoxide (TBHP) were used at room temperature, all epoxidations of β-aryl type substrates proceeded to completion with reasonable reaction times (3.5–6 h). In the case of **7e**, even 5 mol% of **1** promoted the reaction efficiently to give **8a** (yield 73%, 85% ee, entry 2). Other β-aryl type substrates, which have an electron-withdrawing group (entries 5, 6) or an electron donating group (entry 7) on the aromatic ring, were smoothly epoxidized to afford **8g**,**h**, or **8i** in good enantiomeric excess (89–93% ee). This asymmetric catalyst system was also effective for β-alkyl substituted type substrates with higher reactivity than the β-aryl type substrates (entries 8–16). Both primary (entries 8–15) and secondary (entry 16) alkyl substituted substrates gave the products in high yield (72–93%) and slightly lower enantiomeric excess (79–88% ee). Particularly noteworthy is that this reaction was applicable to substrates that were functionalized with a C–C double bond (entries 12–14) or a ketone (entry 15), without overoxidation. To the best of our knowledge, this is the first example of a general catalytic asymmetric epoxidation of α,β-unsaturated carboxylic acid derivatives.

The addition of 3–6 equiv. of $Ph_3P{=}O$ to the lanthanide–BINOL complex also enhances the rate of this reaction. In fact, catalytic asymmetric epoxidation of **7e** and **7j** using the

Table 2. Catalytic asymmetric epoxidation of various α,β-unsaturated carboxylic acid 4-phenylimidazolides using 10 mol% of **1**

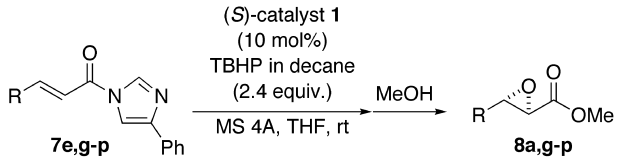

Entry	R	Substrate	Product	Time (h)	Yield (%)	ee (%)
1	Ph–	**7e**	**8a**	3.5	86	92
2[a]		**7e**	**8a**	12	73	85
3[b]		**7e**	**8a**	3.5	85	94
4[c]		**7e**	**8a**	18	47	94
5	4-Cl–C_6H_4–	**7g**	**8g**	5	91	93
6[d]	4-Br–C_6H_4–	**7h**	**8h**	4	86	89
7	4-MeO–C_6H_4–	**7i**	**8i**	6	80	91
8	Ph	**7j**	**8j**	1	86	83
9[b]		**7j**	**8j**	1	84	87
10[c]		**7j**	**8j**	11	58	91
11	Ph	**7k**	**8k**	1	93	79
12		**7l**	**8l**	2	93[e]	86
13		**7m**	**8m**	1.5	92[e]	79
14	Ph	**7n**	**8n**	2	85	82
15	O	**7o**	**8o**	4	81[e]	81
16		**7p**	**8p**	4	72[e]	88

[a] 5 mol% of the catalyst was used.
[b] 30 mol% of $Ph_3P{=}O$ was used instead of 10 mol% of $Ph_3As{=}O$.
[c] Cumene hydroperoxide was used as an oxidant.
[d] 4-Methylimidazolide was used due to the low solubility of the corresponding 4-phenylimidazolide.
[e] Isolated yield of the corresponding peroxycarboxylic acid *tert*-butyl ester.

Table 3. The central metal effects for the epoxidation of **7j** and **7k**

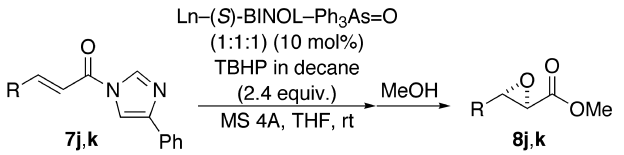

Entry	R	Ln	Time (h)	Yield (%)	ee (%)
1	$Ph(CH_2)_2$–(**7j**)	La (**1**)	1	86	83
2		Pr (**12**)	1.5	87	85
3[a]		Pr (**13**)	4	82	86
4		Sm	6	81	79
5		Gd	3	81	67
6		Dy	3	79	77
7		Yb	20	78	68
8	$Ph(CH_2)_4$–(**7k**)	La (**1**)	1	93	79
9		Pr (**12**)	1.5	88	86
10[a]		Pr (**13**)	7	92	88
11		Sm	5	88	65
12		Gd	8	84	49
13		Dy	2	85	76
14		Yb	18	71	56

[a] 30 mol% of $Ph_3P{=}O$ was used instead of 10 mol% of $Ph_3As{=}O$.

La–BINOL–Ph_3P═O[5] (1:1:3) complex **11** afforded similar results (entries 3, 9). In addition, we examined reactions using cumene hydroperoxide (CMHP) as an oxidant. As shown in entries 4 and 10, the corresponding epoxy esters were obtained with higher selectivity compared to those obtained using TBHP. There was, however, a remarkable decrease in reactivity.

As mentioned above, the β-alkyl substituted type substrates had slightly lower enantioselectivity. To further improve selectivity, the effects of the central metal for the epoxidations of **7j** and **7k** were investigated using 10 mol% of Ln–BINOL–Ph_3As═O complex, generated from Ln(O-*i*-Pr)$_3$, BINOL, and Ph_3As═O in a ratio of 1:1:1. The results are summarized in Table 3. The Pr–BINOL–Ph_3As═O (1:1:1) complex **12** was the best catalyst for both substrates, affording the highest enantioselectivity. The Pr–BINOL–Ph_3P═O (1:1:3) complex **13** was also an effective catalyst with lower reactivity and slightly higher selectivity than **12** (entries 3, 10). In the case of the β-aryl type substrates, the original catalyst La–BINOL–Ph_3As═O (1:1:1) complex **1** gave the best results.

The usefulness of the intermediates **6a** (β-aryl type) and **6j** (β-alkyl type) was demonstrated (Scheme 4). The α,β-epoxy peroxy esters **6a** and **6j** are stable compounds, which were isolated using common flash column chromatography and can be stored at least 2 months in a refrigerator (at 4°C). On the other hand, they are so-called active-esters, thus many kinds of nucleophiles can react very smoothly at the carbonyl carbon in preference to the epoxide. In fact,

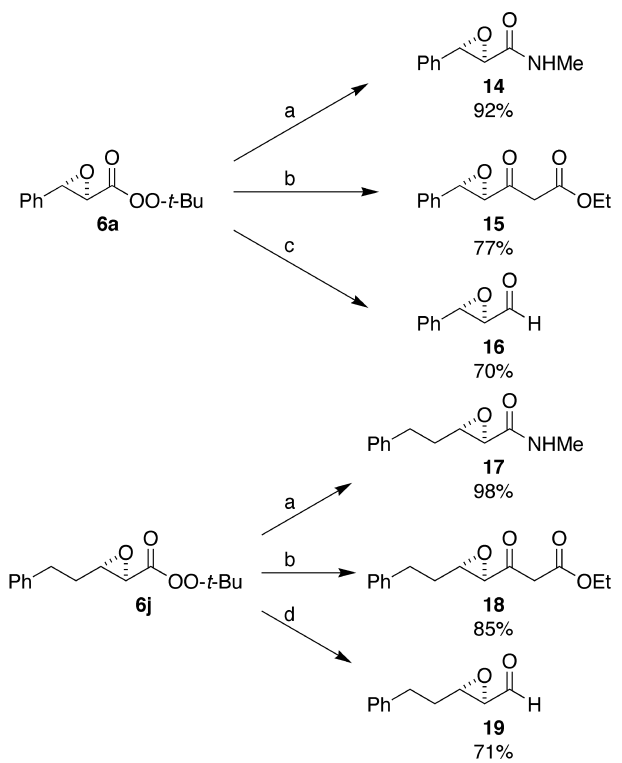

Scheme 4. Further transformations of α,β-epoxy peroxy esters **6a** and **6j**. *Conditions*: (a) methylamine (2.5 equiv.), THF, 0°C; (b) ethyl acetate (2.5 equiv.), LiHMDS (2.0 equiv.), THF, −78°C; (c) Red-Al (0.5 mol equiv.), toluene, −78°C; (d) DIBAL (1.0 equiv.), toluene, −78°C.

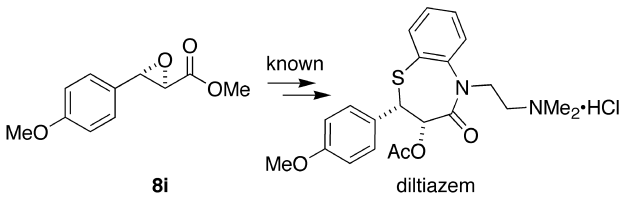

Scheme 5.

they were converted to the corresponding α,β-epoxy amides **14** (93%) and **17** (98%), the γ,δ-epoxy β-keto esters **15** (77%) and **18** (85%), and the α,β-epoxy aldehydes **16** (70%) and **19** (71%) by the addition of amine, lithium ester enolate, and aluminum hydrides (Red-Al or DIBAH), respectively, without any epoxide ring opening reactions.[9] In addition, the epoxide product **8i** is a key intermediate for one of the most potent calcium antagonists diltiazem (Herbesser)[16] (Scheme 5). Further transformation using a tandem process will be discussed in the last section.

2.2. Catalytic asymmetric epoxidation of α,β-unsaturated simple amides

Chiral α,β-epoxy amides are very important compounds because they can be converted into useful chiral building blocks such as α- and β-hydroxy amides. As demonstrated in Scheme 4, many chiral α,β-epoxy amides can be synthesized from the corresponding α,β-epoxy peroxy esters. Catalytic asymmetric epoxidation of α,β-unsaturated amides should be a more direct and efficient method for the preparation of chiral α,β-epoxy amides. There are no reports, however, of catalytic asymmetric epoxidation of α,β-unsaturated amides,[17] perhaps due to the lower reactivity (LUMO energy of *N*-methyl cinnamoyl amide (**20k**): −1.46 eV) than that of α,β-unsaturated ester (−1.70 eV, Table 1, entry 1). While catalytic asymmetric epoxidation of α,β-unsaturated esters proceeded very sluggishly with the use of complex **1**, surprisingly, α,β-unsaturated amides were epoxidized more smoothly under the same conditions. This result prompted us to

Table 4. Effect of the amount of TBHP and the central metal for the epoxidation of **20a**

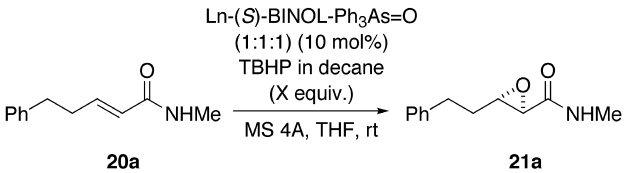

Entry	Ln	TBHP (equiv.)	Time (h)	Yield (%)	ee (%)
1	La (**1**)	1.1	48	29	91
2	La (**1**)	1.2	48	93	97
3	La (**1**)	1.5	48	63	98
4	La (**1**)	2.0	48	57	97
5	La (**1**)	2.4	48	40	94
6	Pr (**12**)	1.2	8	96	99.1
7[a]	Pr (**13**)	1.2	24	48	95
8	Sm (**22**)	1.2 (condition A)	8	97	99.4
9[a]	Sm (**23**)	1.2	24	65	96
10	Gd	1.2	24	71	94
11	Dy	1.2	8	94	98
12	Yb	1.2	24	25	65

[a] 30 mol% of Ph_3P═O was used instead of 10 mol% of Ph_3As═O.

Table 5. Effect of MS 4A for the epoxidation of **20k**

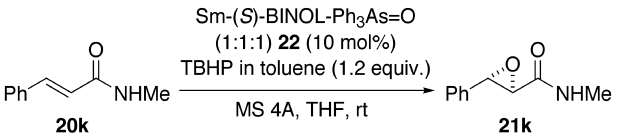

Entry	MS 4A	Additive	Time (h)	Yield (%)	ee (%)
1[a]	not dried	–(condition A)	24	89	99.6
2	dried[b]	H_2O[c]	18	80	99.2
3	dried[b]	–(condition B)	18	95	98.8
4[d]	dried[b]	–	9	92	97.1

[a] Decane solution of TBHP (not dried) was used.
[b] MS 4A was dried for 3 h at 180°C under reduced pressure.
[c] 4 equiv. of H_2O to the catalyst was added.
[d] 30 mol% of Ph_3P═O was used instead of 10 mol% of Ph_3As═O.

optimize the reaction conditions. The effect of the central metal and the amount of TBHP were investigated in detail using **20a** as a representative substrate. The amount of TBHP strongly affected reactivity and 1.2 equiv. of TBHP to **20a** was optimal (Table 4, entry 2). Sm–BINOL–Ph_3As═O complex **22**, generated from Sm(O-*i*-Pr)$_3$, (*S*)-BINOL, and Ph_3As═O in a ratio of 1:1:1, was the best catalyst for this reaction (Table 4, entry 8: condition A).

This condition was also effective for the epoxidation of β-aryl type amides with lower reactivity. To enhance reactivity, further optimization of the reaction was performed. After investigation of the amount of TBHP and the central metal, condition A (Sm–BINOL–Ph_3As═O complex **22** and 1.2 equiv. of TBHP to **20k**) also gave the best result. In these cases, activation of MS 4A was necessary to improve the lower reactivity, but there was a slight decrease in enantiomeric excess (Table 5, entry 4: condition B). Sm–BINOL–Ph_3P═O complex **23** was also effective, however, in the case of epoxidation of α,β-unsaturated simple amides, Ph_3As═O always gave better results (Table 4, entries 7, 9; Table 5, entry 5).

The scope and limitations using numerous substrates were examined. As shown in Table 6, this catalytic system had a broad generality for epoxidations of various β-alkyl and β-aryl type amides. When 5–10 mol% of **22** was used (condition A), β-alkyl type amides **20a–j**, prepared from primary amines (entries 1–5, 10–12), α-branched primary amines (entries 6, 7), and secondary amines (entries 8, 9), were smoothly epoxidized to afford the corresponding α,β-epoxy amides in excellent yield and in excellent enantiomeric excess. The scope and limitations of several β-aryl type amides were also examined using condition B and all cases afforded satisfactory results (entries 13–17). To the best of our knowledge, this is the first example of a general catalytic asymmetric epoxidation of α,β-unsaturated amides.

The nearly optically-pure α,β-epoxy amides obtained were successfully transformed into several useful α- and β-hydroxy carbonyl compounds. Optically-active β-aryl α-hydroxy amides are biologically important structural units and can be easily synthesized from β-aryl α,β-epoxy amides. To achieve efficient transformation, we developed a one-pot tandem catalytic asymmetric epoxidation-Pd-catalyzed epoxide opening process.[10a,18] A representative result is shown in Scheme 6. After completion of the epoxidation,[19] both 5 mol% of Pd–C and MeOH were directly added to the reaction mixture and the mixture was stirred under hydrogen atmosphere. The sequential process functioned efficiently, affording the corresponding α-hydroxy amide **24** in excellent overall yield and enantiomeric excess. In the process, beneficial modifications of the Pd catalyst were achieved by the constituents of the first epoxidation,

Table 6. Catalytic asymmetric epoxidation of various α,β-unsaturated amides

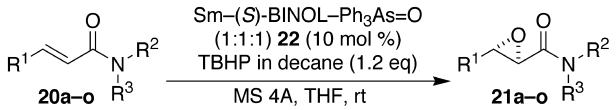

Entry	Substrate			Conditions	Time (h)	Yield (%)	ee (%)
	R^1	NR^2R^3					
1	$Ph(CH_2)_2$	CH_3NH	**20a**	A	8	99	>99
2[a]			**20a**	A	24	94	>99
3	$Ph(CH_2)_2$	BnNH	**20b**	A	6	97	>99
4[a]			**20b**	A	24	82	99
5	$Ph(CH_2)_2$	AllylNH	**20c**	A	4	95	98
6	$Ph(CH_2)_2$	*cyclo*-HexNH	**20d**	A	11	97	>99
7	$Ph(CH_2)_2$	*t*-BuNH	**20e**	A	22	91	99
8	$Ph(CH_2)_2$	$(CH_3)_2N$	**20f**	A	3	96	99
9	$Ph(CH_2)_2$		**20g**	A	4	94	>99
10	$Ph(CH_2)_4$	CH_3NH	**20h**	A	8	81	>99
11	C_3H_7	BnNH	**20i**	A	9	94	94
12	*cyclo*-Hex	BnNH	**20j**	A	12	90	>99
13	Ph	CH_3NH	**20k**	B	18	95	99
14	Ph	BnNH	**20l**	B	18	91	>99
15	Ph	$(CH_3)_2N$	**20m**	B	9	96	>99
16	4-F–C_6H_4	CH_3NH	**20n**	B	20	94	99
17	4-Me–C_6H_4	CH_3NH	**20o**	B	21	89	>99

[a] 5 mol% of the catalyst **22** was used.

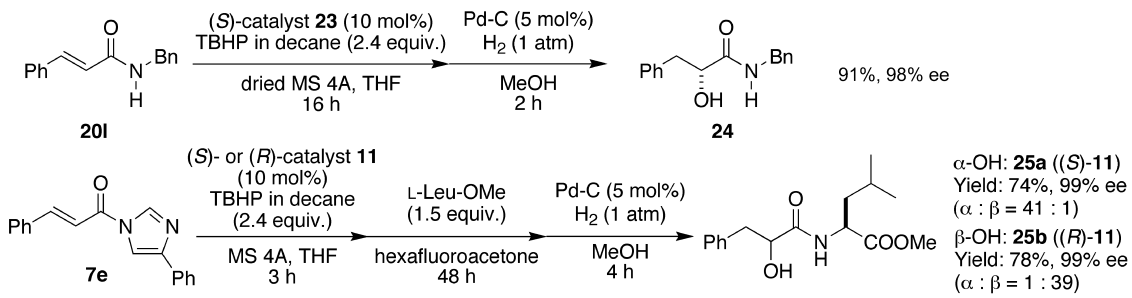

Scheme 6. One-pot tandem catalytic asymmetric epoxidation—Pd-catalyzed epoxide opening process.

producing a more suitable catalyst for the second epoxide opening reaction.[20] This one-pot tandem process was also applied to the syntheses of β-aryl-lactyl-Leu sequences,[21] which can be utilized for the synthesis of a neuropeptide Antho-RNamide (L-3-phenylactyl-Leu-Arg-Asn-NH_2),[21a] using α,β-unsaturated carboxylic acid imidazolide as a starting material. In addition, α,β-epoxy amide was effectively converted to both *syn*- and *anti*-3,5-dihydroxy ester units, which were used for the enantioselective total syntheses of 1,3-polyol/α-pyrone natural products.[10b]

2.3. Mechanistic investigations

Based on X-ray analysis, laser desorption/ionization time-of-flight mass spectrometry, kinetic studies, and asymmetric amplification studies,[4d] asymmetric epoxidation proceeded through internal delivery of *tert*-butyl peroxide from lanthanide metal to the β-carbon of an α,β-unsaturated carbonyl compound, which also coordinated to the lanthanide metal in a *syn-s-cis* manner. Catalytic asymmetric epoxidation of *N*-cinnamoyloxazolidinone (**5**) and α,β-unsaturated Weinreb amide **26** gave unsatisfactory results, which can be explained by the unfavorable *anti* coordination (Scheme 7).

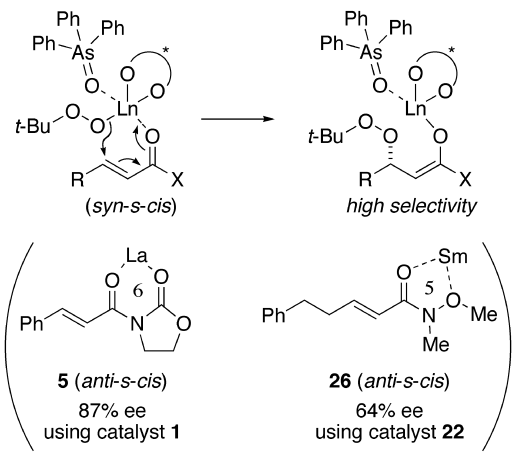

Scheme 7.

Although α,β-unsaturated amide was assumed to have lower reactivity than α,β-unsaturated ester based on the molecular orbital calculations, epoxidation of α,β-unsaturated amide proceeded much more effectively (99% yield, >99% ee) than that of α,β-unsaturated ester (16% yield, 85% ee) (Scheme 8).

In the latter case, the reaction proceeded smoothly in the initial stage then the reactivity rapidly dropped with the color change from pale yellow to black. These results indicated that the LUMO energy of α,β-unsaturated amide and ester are low enough to be promoted epoxidation by Ln–BINOL–Ph_3As=O complex, however, α,β-unsaturated ester promotes deactivation of the lanthanide catalyst. To get insight about these results, we examined the effect of aging of the catalysts (Table 7). When the catalyst was aged for 3 h by adding 1 equiv. of saturated ester **29** (entry 3), nearly same result was obtained compared as that of the control experiment (entry 2). When α,β-unsaturated ester **27** was added to the reaction (entries 4, 5), however, a

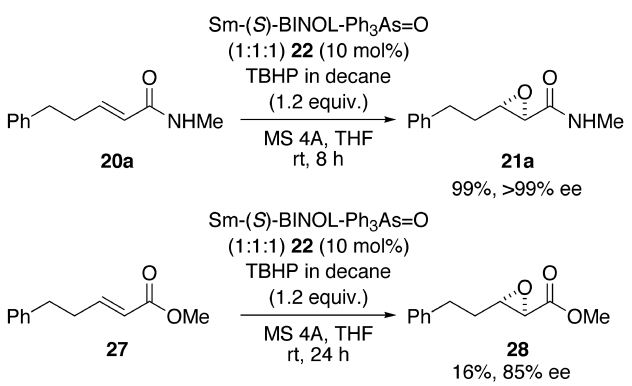

Scheme 8.

Table 7. The effect of aging of the catalyst

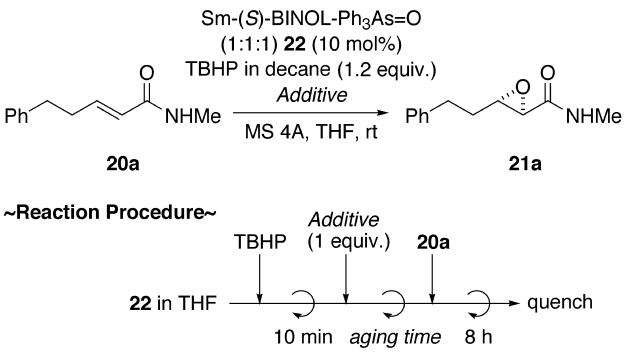

Entry	Additive	Aging time (h)	Yield (%)	ee (%)
1	–	0	99	99.5
2	–	3	99	99.0
3	$Ph(CH_2)_4CO_2Me$ (**29**)	3	99	99.2
4	$Ph(CH_2)_2CH{=}CHCO_2Me$ (**27**)	3	32 (8)[a]	97.1
5	$Ph(CH_2)_2CH{=}CHCO_2Me$ (**27**)	0	62 (0)[a]	99.1

[a] Yield of the α,β-epoxy ester **28**.

decrease in the catalyst activity was observed. These experimental results suggest that α,β-unsaturated ester might form an unfavorable complex with the catalyst, resulting in decreased catalyst activity. Although detailed investigation will be necessary, these finding should be useful to design a novel chiral catalyst system to further improve the epoxidation.

3. Conclusions

We developed the first catalytic asymmetric epoxidation of α,β-unsaturated carboxylic acid derivatives with broad substrate generality via a 1,4-addition of peroxide using α,β-unsaturated carboxylic acid imidazolide as a substrate and the novel lanthanide–BINOL complex as a catalyst. Further, α,β-unsaturated simple amides were good substrates for the epoxidation, affording high enantiomeric excess (up to >99% ee). Moreover, the obtained highly optically active epoxides were successfully transformed into many types of useful chiral compounds such as α,β-epoxy esters, α,β-epoxy amides, α,β-epoxy aldehydes, α,β-epoxy β-keto ester, and α- and β-hydroxy carbonyl compounds. To predict the substrate reactivity, AM1 semiempirical molecular orbital calculation and B3LYP hybrid density functional studies were performed. Although there are some exceptions and further precise calculations are necessary to establish a reliable prediction system, these simple calculations might be useful for initial predictions. Further investigation concerning the development of a catalyst with higher activity, the clarification of the reaction mechanism, and applications to a catalytic asymmetric synthesis of biologically active compounds including a tandem process is ongoing.

4. Experimental

4.1. General

Infrared (IR) spectra were recorded on a JASCO FT/IR 410 Fourier transform infrared spectrophotometer. NMR spectra were recorded on a JEOL JNM-LA500 spectrometer, operating at 500 MHz for ^{1}H NMR and 125.65 MHz for ^{13}C NMR. Chemical shifts in $CDCl_3$ were reported downfield from TMS (=0 ppm) for ^{1}H NMR. For ^{13}C NMR, chemical shifts were reported downfield from TMS (=0 ppm) or on a scale relative to $CHCl_3$ (77.00 ppm for ^{13}C NMR) as an internal reference. Chemical shifts in DMSO-d_6 were reported on a scale relative to DMSO (2.50 ppm for ^{1}H NMR and 39.5 ppm for ^{13}C NMR). Optical rotations were measured on a JASCO P-1010 polarimeter. EI mass spectra were measured on a JEOL JMS-DX303 or JMS-BU20 GCmate. ESI mass spectra were measured on a Waters micromass ZQ Column chromatography was performed with silica gel Merck 60 (230–400 mesh ASTM). The enantiomeric excess was determined by HPLC analysis. HPLC was performed on JASCO HPLC systems consisting of the following: pump, 880-PU or PU-980; detector, 875-UV or UV-970, measured at 254 or 280 nm; column, DAICEL CHIRALPAK AD, AS, AS-H, or OD; mobile phase, hexane-2-propanol; flow rate, 0.4–1.0 mL/min. Reactions were performed in dry solvents under an argon atmosphere, unless otherwise stated. Tetrahydrofuran (THF) was distilled from sodium benzophenone ketyl. All Ln(O-*i*-Pr)$_3$ were purchased from Kojundo Chemical Laboratory Co., LTD., 5-1-28, Chiyoda, Sakado-shi, Saitama 350-0214, Japan (fax: +81-492-84-1351). Powdered molecular sieve 4A (MS 4A) was purchased from Fluka (catalog No. 69836) and used for the epoxidation without drying, unless otherwise stated. Other reagents were purified by the usual methods.

4.2. General procedure for the preparation of α,β-unsaturated carboxylic acid imidazolide 7

1-Ethyl-3-(dimethylaminopropyl)carbodiimide hydrochloride (719 mg, 3.75 mmol) was added to a stirred solution of cinnamic acid (445 mg, 3 mmol) and 4-phenylimidazole (433 mg, 3 mmol) in DMF (15 mL) at room temperature. After stirring for 12 h at the same temperature, the reaction mixture was poured into saturated aqueous ammonium chloride. The resulting mixture was extracted with ethyl acetate (200 mL) and ether (100 mL). The combined organic layers were washed with H_2O (30 mL) followed by brine (30 mL) and dried over Na_2SO_4. After concentration in vacuo, the resulting solid was washed with cold ether to afford imidazolide **7e** (734 mg 90%) as a yellow solid.

Imidazolides **7b–p** were synthesized according to the general procedure. Compounds **5**,[22] **7a**,[23] and **10**[22] were synthesized according to the reported procedure.

4.2.1. 2-Methyl-1-[(2*E*)-1-oxo-3-phenyl-2-propenyl]-1*H*-imidazole (7b). White solid; mp 84–85°C; IR (KBr) ν 3392, 1709, 1618, 1404, 1286, 1254, 1134, 994, 775, 762, 679 cm^{-1}; ^{1}H NMR ($CDCl_3$) δ 2.73 (s, 3H), 6.96 (d, J=1.6 Hz, 1H), 7.05 (d, J=15.3 Hz, 1H), 7.39 (d, J=1.6 Hz, 1H), 7.43–7.49 (m, 3H), 7.62–7.63 (m, 2H), 7.97 (d, J=15.3 Hz, 1H); ^{13}C NMR ($CDCl_3$) δ 17.4, 116.7, 116.9, 128.4, 128.6 (×2), 129.1 (×2), 131.4, 133.8, 148.5, 149.0, 163.7; MS m/z 212 (M^+). HRMS calcd for $C_{13}H_{12}N_2O$ (M^+): 212.0950. Found 212.0959.

4.2.2. 4-Methyl-1-[(2*E*)-1-oxo-3-phenyl-2-propenyl]-1*H*-imidazole (7c). White solid; mp 145–148°C; IR (KBr) ν 3128, 1690, 1626, 1484, 1396, 1376, 1285, 1263, 1174, 987, 763 cm^{-1}; ^{1}H NMR ($CDCl_3$) δ 2.28 (d, J=1.2 Hz, 3H), 7.03 (d, J=15.6 Hz, 1H), 7.33 (br-t, 1H), 7.44–7.47 (m, 3H), 7.63–7.65 (m, 2H), 8.04 (d, J=15.6 Hz, 1H), 8.21 (d, J=1.2 Hz, 1H); ^{13}C NMR ($CDCl_3$) δ 13.6, 112.4, 115.0, 128.6 (×2), 129.1 (×2), 131.5, 133.7, 135.7, 140.7, 149.2, 161.5; MS m/z 212 (M^+). HRMS calcd for $C_{13}H_{12}N_0O$ (M^+): 212.0950. Found 212.0956.

4.2.3. 1-[(2*E*)-1-Oxo-3-phenyl-2-propenyl]-2-phenyl-1*H*-imidazole (7d). White-yellow solid; mp 92–92.5°C; IR (KBr) ν 3383, 1698, 1617, 1465, 1378, 1352, 1230, 1202, 1087, 995, 757, 700 cm^{-1}; ^{1}H NMR ($CDCl_3$) δ 6.48 (d, J=15.3 Hz, 1H), 7.17 (d, J=1.6 Hz, 1H), 7.17–7.19 (m, 2H), 7.30–7.46 (m, 6H), 7.60–7.62 (m, 2H), 7.67 (d, J=1.6 Hz, 1H), 7.82 (d, J=15.3 Hz, 1H); ^{13}C NMR ($CDCl_3$) δ 118.5, 119.3, 128.4 (×2), 128.6 (×2), 128.9 (×2), 129.2, 129.5 (×2), 129.6, 131.3, 131.5, 133.7, 147.7, 148.1, 164.1;

MS *m/z* 274 (M^+). HRMS calcd for $C_{18}H_{14}N_2O$ (M^+): 274.1106. Found 274.1104.

4.2.4. 1-[(2*E*)-1-Oxo-3-phenyl-2-propenyl]-4-phenyl-1*H*-imidazole (7e). Yellow solid; mp 230–232°C; IR (KBr) ν 1687, 1621, 1495, 1395, 1290, 1236, 1188, 988, 753, 694 cm^{-1}; ^1H NMR ($CDCl_3$) δ 7.11 (d, J=15.6 Hz, 1H), 7.31–7.50 (m, 6H), 7.67–7.69 (m, 2H), 7.86–7.87 (m, 2H), 7.91 (d, J=1.6 Hz, 1H), 8.11 (d, J=15.6 Hz, 1H), 8.35 (d, J=1.6 Hz, 1H); ^{13}C NMR ($CDCl_3$) δ 111.2, 114.5, 125.5 (×2), 128.1, 128.8 (×2), 128.9 (×2), 129.9 (×2), 131.8, 132.4, 133.7, 136.3, 143.6, 150.0, 161.6; MS *m/z* 274 (M^+). HRMS calcd for $C_{18}H_{14}N_2O$ (M^+): 274.1106. Found 274.1102.

4.2.5. 1-[(2*E*)-1-Oxo-3-phenyl-2-propenyl]-1*H*-benzoimidazole (7f). White solid; mp 233–234°C; IR (KBr) ν 3091, 1701, 1622, 1506, 1478, 1451, 1319, 1289, 1275, 1225, 1207, 1151, 994, 762 cm^{-1}; ^1H NMR ($CDCl_3$) δ 7.24 (d, J=15.3 Hz, 1H), 7.43–7.50 (m, 5H), 7.68–7.70 (m, 2H), 7.84 (d, J=7.0 Hz, 1H), 8.11 (d, J=15.3 Hz, 1H), 8.34 (d, J=7.0 Hz, 1H), 8.57 (s, 1H); ^{13}C NMR ($CDCl_3$) δ 115.7, 115.8, 120.6, 125.1, 125.8, 128.7 (×2), 129.2 (×2), 131.5, 131.9, 133.8, 140.7, 144.1, 148.9, 162.9; MS *m/z* 248 (M^+). Anal. calcd for $C_{16}H_{12}N_2O$: C, 77.40; H, 4.87; N, 11.28. Found: C, 77.24; H, 5.01; N, 11.05.

4.2.6. 1-[(2*E*)-3-(4-Chlorophenyl)-1-oxo-2-propenyl]-4-phenyl-1*H*-imidazole (7g). White-yellow solid; mp 269–270°C; IR (KBr) ν 3127, 1697, 1620, 1492, 1409, 1390, 1190, 993, 980, 823, 784, 762, 694, 419 cm^{-1}; ^1H NMR (DMSO-d_6) δ 7.27–7.31 (m, 1H), 7.40–7.43 (m, 2H), 7.58 (m, 2H), 7.72 (d, J=15.6 Hz, 1H), 7.90–7.92 (m, 2H), 7.98 (m, 2H), 8.01 (d, J=15.6 Hz, 1H), 8.42 (s, 1H), 8.81 (s, 1H); ^{13}C NMR (DMSO-d_6) δ 112.1, 117.1, 125.1 (×2), 127.7, 128.8 (×2), 129.2 (×2), 131.0 (×2), 132.8, 133.0, 136.1, 137.9, 142.4, 147.0, 161.8; MS *m/z* 308 (M^+). HRMS calcd for $C_{18}H_{13}ClN_2O$ (M^+): 308.0716. Found 308.0714.

4.2.7. 1-[(2*E*)-3-(4-Bromophenyl)-1-oxo-2-propenyl]-4-methyl-1*H*-imidazole (7h). Yellow solid; mp 203–205°C; IR (KBr) ν 3127, 1692, 1624, 1585, 1483, 1406, 1392, 1278, 1261, 1175, 987, 820, 781, 403 cm^{-1}; ^1H NMR ($CDCl_3$) δ 2.28 (d, J=1.2 Hz, 3H), 7.04 (d, J=15.6 Hz, 1H), 7.33 (dd, J=1.2, 1.2 Hz, 1H), 7.50–7.52 (m, 2H), 7.58–7.60 (m, 2H), 7.97 (d, J=15.6 Hz, 1H), 8.24 (d, J=1.2 Hz, 1H); ^{13}C NMR ($CDCl_3$) δ 13.6, 112.4, 115.5, 126.0, 130.0 (×2), 132.4 (×2), 132.6, 135.6, 140.7, 147.8, 161.3; MS *m/z* 292 (M^+), 290 (M^+). Anal. calcd for $C_{13}H_{11}BrN_2O$: C, 53.63; H, 3.81; N, 9.62. Found: C, 53.61; H, 3.91; N, 9.39.

4.2.8. 1-[(2*E*)-3-(4-Methoxyphenyl)-1-oxo-2-propenyl]-4-phenyl-1*H*-imidazole (7i). White-yellow solid; mp 188–189°C; IR (KBr) ν 3120, 1695, 1621, 1560, 1572, 1511, 1294, 1250, 1174, 997, 978, 834, 766, 697 cm^{-1}; ^1H NMR ($CDCl_3$) δ 3.88 (s, 3H), 6.96 (d, J=15.6 Hz, 1H), 6.97 (m, 2H), 7.30–7.44 (m, 3H), 7.63 (m, 2H), 7.85–7.90 (m, 2H), 7.90 (d, J=1.2 Hz, 1H), 8.06 (d, J=15.6 Hz, 1H), 8.33 (d, J=1.2 Hz, 1H); ^{13}C NMR ($CDCl_3$) δ 55.5, 111.2, 111.8, 114.7 (×2), 125.4 (×2), 126.5, 127.9, 128.7 (×2), 130.8 (×2), 132.7, 136.3, 143.6, 149.6, 161.9, 162.6; MS *m/z* 304 (M^+). Anal. calcd for $C_{19}H_{16}N_2O_2$: C, 74.98; H, 5.30; N, 9.20. Found: C, 75.01; H, 5.38; N, 9.09.

4.2.9. 1-[(2*E*)-1-Oxo-5-phenyl-2-pentenyl]-4-phenyl-1*H*-imidazole (7j). White solid; mp 140–144°C; IR (KBr) ν 1698, 1635, 1496, 1396, 1196, 758, 697, 409 cm^{-1}; ^1H NMR ($CDCl_3$) δ 2.73 (ddd, J=14.5, 7.4, 1.5 Hz, 2H), 2.90 (t, J=7.4 Hz, 2H), 6.48 (dd, J=15.3, 1.5 Hz, 1H), 7.21–7.44 (m, 9H), 7.76 (d, J=1.2 Hz, 1H), 7.82 (m, 2H), 8.15 (d, J=1.2 Hz, 1H); ^{13}C NMR ($CDCl_3$) δ 34.1, 34.4, 111.0, 119.6, 125.4 (×2), 126.5, 127.9, 128.4 (×2), 128.6 (×2), 128.7 (×2), 132.6, 136.3, 140.1, 153.9, 161.2; MS *m/z* 302 (M^+). HRMS calcd for $C_{20}H_{18}N_2O$ (M^+): 302.1419. Found 302.1418.

4.2.10. 1-[(2*E*,6*Z*)-1-Oxo-2,6-octadienyl]-4-phenyl-1*H*-imidazole (7l). White solid; mp 96–102°C; IR (KBr) ν 3132, 3008, 1702, 1642, 1503, 1398, 1312, 1295, 1254, 1200, 978, 758, 689 cm^{-1}; ^1H NMR ($CDCl_3$) δ 1.64–1.66 (m, 3H), 2.32–2.35 (m, 2H), 2.45–2.49 (m, 2H), 5.39–5.41 (m, 1H), 5.55–5.59 (m, 1H), 6.56 (dt, J=15.3, 1.5 Hz, 1H), 7.30–7.43 (m, 3H), 7.41 (dt, J=15.3, 7.0 Hz, 1H), 7.82 (d, J=1.2 Hz, 1H), 7.82–7.84 (m, 2H), 8.24 (d, J=1.2 Hz, 1H); ^{13}C NMR ($CDCl_3$) δ 12.9, 25.2, 32.8, 111.1, 119.1, 125.4 (×2), 125.8, 127.9, 128.2, 128.7 (×2), 132.6, 136.3, 143.7, 154.9, 161.3; MS *m/z* 266 (M^+). HRMS calcd for $C_{17}H_{18}N_2O$ (M^+): 266.1419. Found 266.1416.

4.2.11. 1-[(2*E*,6*E*)-1-Oxo-2,6-octadienyl]-4-phenyl-1*H*-imidazole (7m). White-yellow solid; mp 112–119°C; IR (KBr) ν 3133, 2934, 1698, 1635, 1499, 1395, 1293, 1253, 1201, 983, 964, 758, 691 cm^{-1}; ^1H NMR ($CDCl_3$) δ 1.68 (dd, J=6.1, 1.2 Hz, 3H), 2.23–2.27 (m, 2H), 2.42–2.47 (m, 2H), 5.40–5.45 (m, 1H), 5.49–5.56 (m, 1H), 6.56 (dt, J=15.3, 1.5 Hz, 1H), 7.29–7.42 (m, 3H), 7.39 (dt, J=15.3, 7.0 Hz, 1H), 7.82 (d, J=1.2 Hz, 1H), 7.82–7.84 (m, 2H), 8.24 (d, J=1.2 Hz, 1H); ^{13}C NMR ($CDCl_3$) δ 17.9, 30.8, 32.9, 111.1, 119.0, 125.3 (×2), 126.8, 127.9, 128.7 (×2), 129.0, 132.5, 136.4, 143.6, 155.0, 161.3; MS *m/z* 266 (M^+). HRMS calcd for $C_{17}H_{18}N_2O$ (M^+): 266.1419. Found 266.1424.

4.2.12. 1-[(2*E*,6*Z*)-1-Oxo-7-phenyl-2,6-heptadienyl]-4-phenyl-1*H*-imidazole (7n). White-yellow solid; mp 117–119°C; IR (KBr) ν 3127, 1699, 1643, 1498, 1401, 1254, 1204, 758, 695 cm^{-1}; ^1H NMR ($CDCl_3$) δ 2.52–2.56 (m, 2H), 2.61–2.65 (m, 2H), 5.65 (dt, J=11.6, 7.0 Hz, 1H), 6.50 (dt, J=15.3, 1.6 Hz, 1H), 6.54 (d, J=11.6 Hz, 1H), 7.29–7.42 (m, 9H), 7.77 (d, J=1.2 Hz, 1H), 7.81–7.83 (m, 2H), 8.17 (d, J=1.2 Hz, 1H); ^{13}C NMR ($CDCl_3$) δ 26.6, 32.9, 111.1, 119.3, 125.4 (×2), 127.0, 127.9, 128.4 (×2), 128.7 (×2), 128.7 (×2), 130.2, 130.6, 132.6, 136.4, 137.1, 143.7, 154.3, 161.2; MS *m/z* 328 (M^+). HRMS calcd for $C_{22}H_{20}N_2O$ (M^+): 328.1576. Found 328.1577.

4.2.13. 1-[(2*E*)-1,7-Dioxo-2-octenyl]-4-phenyl-1*H*-imidazole (7o). White-yellow solid; IR (KBr) ν 3136, 1707, 1697, 1637, 1316, 1295, 1252, 1199, 989, 858, 767, 698 cm^{-1} ^1H NMR ($CDCl_3$) δ 1.84 (tt, J=7.0 Hz, 7.0 Hz, 2H), 2.16 (s, 3H), 2.38–2.42 (m, 2H), 2.54 (t, J=7.0 Hz, 2H), 6.57 (dt, J=15.3, 1.6 Hz, 1H), 7.30–7.43 (m, 3H), 7.38 (dt, J=15.3, 7.0 Hz, 1H), 7.82 (d, J=1.5 Hz, 1H), 7.82–7.84 (m, 2H), 8.25 (d, J=1.5 Hz, 1H); ^{13}C NMR ($CDCl_3$) δ 21.6, 30.0, 32.0, 42.4, 111.0, 119.3, 125.4 (×2), 127.9, 128.7 (×2), 132.5, 136.4, 143.7, 154.3, 161.2, 207.7; MS *m/z* 282 (M^+). HRMS calcd for $C_{17}H_{18}N_2O_2$ (M^+): 282.1368. Found 282.1365.

4.2.14. 1-[(2*E*)-3-Cyclohexyl-1-oxo-2-propenyl]-1*H*-imidazole (7p). White solid; mp 147–149°C; IR (KBr) ν 3129, 2931, 2855, 1698, 1627, 1495, 1389, 1279, 1246, 1197, 1177, 987, 762, 692 cm^{-1}; ^1H NMR ($CDCl_3$) δ 1.19–1.40 (m, 6H), 1.71–1.88 (m, 4H), 2.32–2.35 (m, 1H), 6.48 (dd, J=15.3, 1.2 Hz, 1H), 7.30–7.43 (m, 3H), 7.36 (dd, J=15.3, 7.0 Hz, 1H), 7.82 (d, J=1.2 Hz, 1H), 7.82–7.84 (m, 2H), 8.24 (d, J=1.2 Hz, 1H); ^{13}C NMR ($CDCl_3$) δ 25.6, 25.8, 31.5, 41.3, 111.1, 116.4, 125.4 (×2), 127.9, 128.7 (×2), 132.6, 136.4, 143.7, 160.4, 161.7; MS m/z 280 (M^+). HRMS calcd for $C_{18}H_{20}N_2O$: 280.1576. Found 280.1574.

4.3. General procedure for the catalytic asymmetric epoxidation of α,β-unsaturated carboxylic acid imidazolide 7 to synthesize the α,β-epoxy esters 8

A solution of La(O-*i*-Pr)$_3$ (0.125 mL, 0.025 mmol, 0.2 M solution in THF) was added to a mixture of (*S*)-BINOL (7.2 mg, 0.025 mmol), triphenylarsine oxide (8.1 mg, 0.025 mmol) and MS 4A (250 mg) in dry THF (2.5 mL) at room temperature. After stirring for 45 min at the same temperature, TBHP (0.12 mL, 0.6 mmol, 5 M solution in decane) was added. After stirring for 10 min, imidazolide **7e** (68.6 mg, 0.25 mmol) was added directly and the mixture was stirred at room temperature. After the starting material was completely consumed, excess MeOH (0.5 mL) was added to the reaction mixture and the resulting mixture was stirred for 3 h, and then quenched by the addition of 1% aqueous citric acid solution (2.5 mL) at 0°C. The mixture was extracted with ethyl acetate (2×10 mL) and the combined organic layers were washed with 2% aqueous sodium thiosulfate (5 mL) and brine (5 mL), and dried over Na_2SO_4. After concentration in vacuo, the residue was purified by flash column chromatography (SiO_2, hexane/ethyl acetate 50:1) to give epoxy ester **8a** (38.5 mg, 86%) as a colorless oil.

4.3.1. Methyl (2*R*,3*S*)-3-phenyloxiranecarboxylate (8a).[7a,b] White solid; $[\alpha]_D^{24}=-111.8$ (c 1.17, $CHCl_3$, 92% ee). The enantiomeric excess was determined by chiral stationary-phase HPLC analysis (DAICEL CHIRALPAK AD, *i*-PrOH/hexane 2:98, flow rate 0.4 mL/min, t_R 28.6 min (2*S*,3*R*)-isomer and 30.6 min (2*R*,3*S*)-isomer, detection at 254 nm).

4.3.2. Methyl (2*R*,3*S*)-3-(4-chlorophenyl)oxiranecarboxylate (8g). White-yellow solid; mp 59–62°C; IR (neat) ν 3034, 1753, 1496, 1427, 1340, 1213, 1090, 834, 802, 728 cm^{-1}; ^1H NMR ($CDCl_3$) δ 3.47 (dd, J=1.9, 1.5 Hz, 1H), 3.83 (s, 3H), 4.08 (d, J=1.5 Hz, 1H), 7.21–7.23 (m, 2H), 7.33–7.35 (m, 2H); ^{13}C NMR ($CDCl_3$) δ 52.7, 56.6, 57.3, 127.1 (×2), 128.9 (×2), 133.4, 134.9, 168.3; MS m/z 212 (M^+), 155. HRMS calcd for $C_{10}H_9ClO_3$ (M^+): 212.0240. Found 212.0246; $[\alpha]_D^{23}=-148.7$ (c 1.03, $CHCl_3$, 93% ee). The enantiomeric excess was determined by chiral stationary-phase HPLC analysis (DAICEL CHIRALCEL OD, *i*-PrOH/hexane 1:9, flow rate 0.5 mL/min, t_R 14.7 min (major-isomer) and 17.7 min (minor-isomer), detection at 254 nm).

4.3.3. Methyl (2*R*,3*S*)-3-(4-bromophenyl)oxiranecarboxylate (8h). White-yellow solid; mp 74–75°C; IR (neat) ν 3033, 1752, 1493, 1425, 1339, 1214, 1071, 832, 801, 724 cm^{-1}; ^1H NMR ($CDCl_3$) δ 3.47 (d, J=1.4 Hz, 1H), 3.83 (s, 3H), 4.07 (d, J=1.4 Hz, 1H), 7.15–7.17 (m, 2H), 7.49–7.51 (m, 2H); ^{13}C NMR ($CDCl_3$) δ 52.7, 56.6, 57.4, 123.1, 127.4 (×2), 131.9 (×2), 134.0, 168.3; MS m/z 255 (M^+), 200, 198. Anal. calcd for $C_{10}H_9BrO_3$: C, 46.72; H, 3.53. Found: C, 46.47; H, 3.57; $[\alpha]_D^{25}=-118.0$ (c 0.79, $CHCl_3$, 89% ee). The enantiomeric excess was determined by chiral stationary-phase HPLC analysis (DAICEL CHIRALCEL OD, *i*-PrOH/hexane 1:9, flow rate 0.5 mL/min, t_R 15.1 min (major-isomer) and 18.8 min (minor-isomer), detection at 254 nm).

4.3.4. Methyl (2*R*,3*S*)-3-(4-methoxyphenyl)oxiranecarboxylate (8i).[7c] Because of the instability of the compound **8i** against acidic conditions, special work-up and purification methods were necessary to minimize the decomposition of **8i** to the corresponding α,β-dihydroxy ester. After conversion of the peroxy ester to the methyl ester **8i**, the reaction mixture was cooled at 0°C, diluted with ethyl acetate (5 mL), and then quenched by the addition of aqueous 0.01 M HCl solution (10 mL) to the mixture. The resulting mixture was poured into water (5 mL) and extracted with ethyl acetate (2×15 mL). The combined organic layers were washed with 2% aqueous sodium thiosulfate (5 mL) and brine (5 mL), and dried over Na_2SO_4. After concentration in vacuo, the residue was purified by flash column chromatography (neutral SiO_2, hexane/ethyl acetate/triethylamine 200:10:1) to give **8i** in 80% isolated yield as a colorless oil. $[\alpha]_D^{25}=-144.8$ (c 0.63, $CHCl_3$, 91% ee). The enantiomeric excess was determined by chiral stationary-phase HPLC analysis (DAICEL CHIRALCEL OD, *i*-PrOH/hexane 1:9, flow rate 1.0 mL/min, t_R 8.5 min (2*R*,3*S*)-isomer and 12.1 min (2*S*,3*R*)-isomer, detection at 254 nm).

4.3.5. Methyl (2*R*,3*S*)-3-(2-phenylethyl)oxiranecarboxylate (8j). Colorless oil; IR (neat) ν 3027, 2952, 1752, 1453, 1291, 1029, 700 cm^{-1}; ^1H NMR ($CDCl_3$) δ 1.86–2.01 (m, 2H), 2.73–2.86 (m, 2H), 3.20 (ddd, J=6.4, 4.6, 1.8 Hz, 1H), 3.21 (4.07 (d, J=1.8 Hz, 1H), 3.76 (s, 3H), 7.18–7.31 (m, 5H); ^{13}C NMR ($CDCl_3$) δ 31.9, 33.2, 52.4, 53.1, 57.8, 126.3, 128.3 (×2), 128.6 (×2), 140.5, 169.5; MS m/z 206 (M^+). HRMS calcd for $C_{12}H_{14}O_3$ (M^+): 206.0943. Found 206.0945; $[\alpha]_D^{25}=-33.5$ (c 0.82, $CHCl_3$, 83% ee). The enantiomeric excess was determined by chiral stationary-phase HPLC analysis (DAICEL CHIRALPAK AD, *i*-PrOH/hexane 2:98, flow rate 1.0 mL/min, t_R 9.7 min (2*R*,3*S*)-isomer and 10.7 min (2*S*,3*R*)-isomer, detection at 254 nm).

4.3.6. Methyl (2*R*,3*S*)-3-(4-pentenylbutyl)oxiranecarboxylate (8k). Pale yellow oil; IR (neat) ν 3025, 2935, 2858, 1755, 1453, 1291, 1250, 1030, 700 cm^{-1}; ^1H NMR ($CDCl_3$) δ 7.34 (m, 2H), 7.24 (m, 3H), 3.84 (s, 3H), 3.29 (d, J=2 Hz, 1H), 3.22 (ddd, J=6, 5, 2 Hz, 1H), 2.69 (t, J=7.5 Hz, 2H), 1.78–1.55 (m, 6H); ^{13}C NMR ($CDCl_3$) δ 169.7, 142.1, 128.34 (×2), 128.29 (×2), 125.8, 58.4, 52.9, 52.4, 35.7, 31.3, 31.0, 25.3; EI-MS m/z 234 (M^+); $[\alpha]_D^{24}=-24.6$ (c 1.7, $CHCl_3$, 99% ee). The enantiomeric excess was determined by chiral stationary-phase HPLC analysis (DAICEL CHIRALPAK AD-H, *i*-PrOH/hexane 1:99, flow rate 1.0 mL/min, t_R 12.1 min (2*R*,3*S*)-isomer and 14.0 min (2*S*,3*R*)-isomer, detection at 254 nm).

4.3.7. Methyl (2*R*,3*S*)-3-[(3*Z*)-3-pentenyl]oxiranecarboxylate (8l). Colorless oil; IR (neat) ν 3015, 2953, 1755, 1446, 1291, 1206, 1030, 711 cm^{-1}; ^1H NMR ($CDCl_3$) δ 1.62 (ddd, J=6.7, 1.8, 0.9 Hz, 3H), 1.64–1.73 (m, 2H), 2.21–2.25 (m, 2H), 3.18 (ddd, J=6.1, 5.2, 1.8 Hz, 1H), 3.25 (d, J=1.8 Hz, 1H), 3.78 (s, 3H), 5.36–5.42 (m, 1H), 5.44–5.56 (m, 1H); ^{13}C NMR ($CDCl_3$) δ 12.7, 23.0, 31.3, 52.4, 53.0, 58.1, 125.4, 128.4, 169.7; MS *m/z* 149, 137, 121. HRMS calcd for $C_9H_{13}O_3$ (M^+-1): 169.0865. Found 169.0861; $[\alpha]_D^{21}=-14.8$ (*c* 1.09, $CHCl_3$, 86% ee). The enantiomeric excess was determined by chiral stationary-phase HPLC analysis (DAICEL CHIRALCEL OD, *i*-PrOH/hexane 1:9, flow rate 0.5 mL/min, t_R 14.5 min (minor-isomer) and 23.7 min (major-isomer), detection at 254 nm) after conversion to the corresponding 4-methoxybenzyl ester.

4.3.8. Methyl (2*R*,3*S*)-3-[(3*E*)-3-pentenyl]oxiranecarboxylate (8m). Colorless oil; IR (neat) ν 2938, 2856, 1755, 1448, 1291, 1206, 1029, 968, 471 cm^{-1}; ^1H NMR ($CDCl_3$) δ 1.62 (dd, J=6.1 Hz, 1.2 Hz, 3H), 1.60–1.73 (m, 2H), 2.12–2.20 (m, 2H), 3.17 (ddd, J=6.1, 5.2, 1.8 Hz, 1H), 3.25 (d, J=1.8 Hz, 1H), 3.78 (s, 3H), 5.36–5.42 (m, 1H), 5.44–5.56 (m, 1H); ^{13}C NMR ($CDCl_3$) δ 17.8, 28.7, 31.4, 52.4, 53.0, 58.1, 126.4, 129.3, 169.7; MS *m/z* 149, 137, 121, 120. HRMS calcd for $C_6H_9O_3$ ($M^+-C_3H_5$): 129.0552. Found 129.0562; $[\alpha]_D^{23}=-21.2$ (*c* 0.9, $CHCl_3$, 79% ee). The enantiomeric excess of **6n** was determined by chiral stationary-phase HPLC analysis (DAICEL CHIRALPAK AD, *i*-PrOH/hexane 1:9, flow rate 0.5 mL/min, t_R 14.5 min (minor-isomer) and 20.4 min (major-isomer), detection at 254 nm) after conversion to the corresponding 4-methoxybenzyl ester.

4.3.9. Methyl (2*R*,3*S*)-3-[(3*Z*)-4-phenyl-3-butenyl]oxiranecarboxylate (8n). Colorless oil; IR (neat) ν 3019, 2952, 1753, 1446, 1291, 1206, 1029, 770, 701 cm^{-1}; ^1H NMR ($CDCl_3$) δ 1.70–1.84 (m, 2H), 2.49–2.54 (m, 2H), 3.19 (ddd, J=6.4, 4.9, 1.9 Hz, 1H), 3.25 (d, J=1.9 Hz, 1H), 3.76 (s, 3H), 5.65 (dt, J=11.6, 7.3 Hz, 1H), 6.48 (d, J=11.6 Hz, 1H), 7.22–7.26 (m, 2H), 7.32–7.35 (m, 3H); ^{13}C NMR ($CDCl_3$) δ 24.8, 31.6, 52.4, 52.9, 57.9, 126.8, 128.2 (×2), 128.7 (×2), 130.2, 130.4, 137.1, 169.5; MS *m/z* 232 (M^+). HRMS calcd for $C_{14}H_{16}O_3$ (M^+): 232.1099. Found 232.1098; $[\alpha]_D^{22}=-13.7$ (*c* 0.54, $CHCl_3$, 82% ee). The enantiomeric excess was determined by chiral stationary-phase HPLC analysis (DAICEL CHIRALCEL OD, *i*-PrOH/hexane 1:9, flow rate 0.5 mL/min, t_R 14.9 min (minor-isomer) and 25.8 min (major-isomer), detection at 254 nm).

4.3.10. Methyl (2*R*,3*S*)-3-(4-oxopentyl)oxiranecarboxylate (8o). Colorless oil; IR (neat) ν 2955, 1751, 1714, 1488, 1361, 1293, 1207 cm^{-1}; ^1H NMR ($CDCl_3$) δ 1.49–1.58 (m, 1H), 1.69–1.82 (m, 3H), 2.15 (s, 1H), 2.52 (t, J=7.3 Hz, 2H), 3.16 (ddd, J=6.7, 4.0, 1.8 Hz, 1H), 3.22 (d, J=1.8 Hz, 1H), 3.78 (s, 3H); ^{13}C NMR ($CDCl_3$) δ 19.8, 30.0, 30.6, 42.6, 52.4, 52.6, 58.1, 169.5, 208.0; MS *m/z* 186 (M^+). HRMS calcd for $C_9H_{14}O_4$ (M^+): 186.0892. Found 186.0888; $[\alpha]_D^{22}=-10.3$ (*c* 0.26, $CHCl_3$, 81% ee). The enantiomeric excess was determined by chiral stationary-phase HPLC analysis (DAICEL CHIRALCEL OD, *i*-PrOH/hexane 1:3, flow rate 0.5 mL/min, t_R 19.7 min (minor-isomer) and 30.3 min (major-isomer), detection at 254 nm) after conversion to the corresponding 4-methoxybenzyl ester.

4.3.11. Methyl (2*R*,3*S*)-3-cyclohexyloxiranecarboxylate (8p).[24] Colorless oil; $[\alpha]_D^{25}=-24.8$ (*c* 1.27, $CHCl_3$, 88% ee). The enantiomeric excess was determined by chiral stationary-phase HPLC analysis (DAICEL CHIRALPAK AD, *i*-PrOH/hexane 1:9, flow rate 0.5 mL/min, t_R 15.5 min (2*S*,3*R*)-isomer and 17.5 min (2*R*,3*S*)-isomer, detection at 254 nm) after conversion to the corresponding 4-methoxybenzyl ester.

4.3.12. *tert*-Butyl (2*R*,3*S*)-3-phenylperoxyglycidate (6a). After completion of the epoxidation, the reaction was quenched by the addition of 1% aqueous citric acid solution (2.5 mL) at 0°C. The mixture was extracted with ethyl acetate (2×10 mL) and the combined organic layers were washed with brine (5 mL) and dried over Na_2SO_4. After concentration in vacuo, the residue was purified by flash column chromatography (SiO_2, hexane/ethyl acetate 50:1) to give **6a** (51.0 mg, 86%) as a white solid: mp 86–88°C; IR (neat) ν 2983, 1787, 1458, 1419, 1367, 1248, 1187, 1131, 752, 697 cm^{-1}; ^1H NMR ($CDCl_3$) δ 1.34 (s, 9H), 3.52 (d, J=2.0 Hz, 1H), 4.14 (d, J=2.0 Hz, 1H), 7.23–7.28 (m, 2H), 7.33–7.39 (m, 3H); ^{13}C NMR ($CDCl_3$) δ 26.1 (×3), 54.9, 58.1, 84.5, 125.8 (×2), 128.7 (×2), 129.2, 134.4, 165.8; MS *m/z* 236 [M^+]; $[\alpha]_D^{27}=-167.2$ (*c* 0.75, $CHCl_3$, 94% ee). HRMS calcd for $C_{13}H_{16}O_4$ (M^+): 236.1049. Found 236.1055.

4.3.13. The absolute configurations of 8. The absolute configurations of the epoxy ester **8a**,[7a,b] **8i**,[7c] and **8p**[24] were determined by comparing the measured optical rotations with the reported ones. The absolute configuration of **8g** was determined by comparing the measured optical rotation with the reported rotation[25] after converting into the corresponding β-hydroxy ester. The absolute configuration of **8k** was determined by Mosher's method after conversion to the corresponding β-hydroxy ester.[26] The absolute configurations of **8l** and **8m** were determined by comparing the measured optical rotation with the reported rotation[27] after converting into methyl 3-hydroxyoctanoate.

4.4. General procedure for the catalytic asymmetric epoxidation of β-alkyl type α,β-unsaturated amides (condition A)

A solution of Sm(O-*i*-Pr)$_3$ (0.5 mL, 0.05 mmol, 0.1 M solution in THF) was added to a mixture of (*S*)-BINOL (14.3 mg, 0.05 mmol), triphenylarsine oxide (16.1 mg, 0.05 mmol) and MS 4A (500 mg) in dry THF (5 mL) at room temperature. After stirring for 45 min at the same temperature, TBHP (0.12 mL, 0.6 mmol, 5 M solution in decane) was added. After stirring for 10 min, amide **20a** (94.6 mg, 0.5 mmol) was added directly and the mixture was stirred at room temperature. After complete consumption of the starting material (8 h), the reaction mixture was diluted with ethyl acetate (20 mL) and quenched with 2% aqueous citric acid (5 mL). The water layer was extracted with ethyl acetate (10 mL), and the combined organic layers were washed with brine (10 ml) and dried over Na_2SO_4. After concentration in vacuo, the residue was purified by flash chromatography (SiO_2, hexane/ethyl acetate=4:1–3:1)

to give epoxy amide **21a** (101.9 mg, 99%) as a white yellow solid.

4.4.1. (2*R*,3*S*)-3-Phenethyloxirane-2-carboxlic acid methyamine (21a). White yellow solid; IR (KBr) ν 3294, 3124, 1656, 1580, 1450, 1267, 902, 742, 695 cm^{-1}; ^1H NMR ($CDCl_3$) δ 1.80–1.81 (m, 1H), 1.99–2.06 (m, 4H), 2.73–2.83 (m, 2H), 2.79 (d, J=5.0 Hz, 3H), 2.96 (ddd, J=6.6, 4.3, 2.1 Hz, 1H), 3.23 (d, J=2.1 Hz, 1H), 6.09 (br-s, 1H), 7.19–7.23 (m, 3H), 7.27–7.33 (m, 2H); ^{13}C NMR ($CDCl_3$) δ 25.7, 32.0, 33.7, 55.7, 59.2, 126.5, 128.6 (×2), 128.8 (×2), 140.7, 169.2; ESI-MS m/z 228 ($M+Na^+$). HRMS calcd for $C_{12}H_{15}NO_2$ (M^+): 205.1103. Found 205.1111. The enantiomeric excess was determined by chiral stationary-phase HPLC analysis (DAICEL CHIRALPAK AS-H, *i*-PrOH/hexane 1:4, flow rate 0.6 mL/min, t_R 26.0 min ((2*S*,3*R*)-isomer) and 35.5 min ((2*R*,3*S*)-isomer), detection at 254 nm); $[\alpha]_D^{27}$=+12.2 (*c* 1.50, $CHCl_3$, >99% ee).

4.4.2. (2*R*,3*S*)-3-Phenethyloxirane-2-carboxlic acid benzylamide (21b). White solid; IR (KBr) ν 3262, 3054, 1654, 1566, 1495, 1454, 1423, 1223, 900, 719, 697 cm^{-1}; ^1H NMR ($CDCl_3$) δ 1.83–1.89 (m, 1H) 1.98–2.05 (m, 1H), 2.73–2.83 (m, 2H), 2.99 (ddd, J=6.5, 4.6, 2.1 Hz, 1H), 3.30 (d, J=2.1 Hz, 1H), 4.38 (dd, J=14.7, 5.8 Hz, 1H), 4.42 (dd, J=14.7, 5.8 Hz, 1H), 6.39 (br-s, 1H), 7.05–7.37 (m, 10H); ^{13}C NMR ($CDCl_3$) δ 31.8, 33.4, 42.8, 55.4, 59.0, 126.2, 127.6, 127.7 (×2), 128.3 (×2), 128.6 (×2), 128.7 (×2), 137.6, 140.4, 168.2; ESI-MS m/z 304 ($M+Na^+$). HRMS calcd for $C_{18}H_{19}NO_2$ (M^+): 281.1416. Found 281.1421. The enantiomeric excess was determined by chiral stationary-phase HPLC analysis (DAICEL CHIRALPAK AS-H, *i*-PrOH/hexane 1:4, flow rate 0.8 mL/min, t_R 28.4 min ((*2S,3R*)-isomer) and 50.5 min ((*2R,3S*)-isomer), detection at 254 nm); $[\alpha]_D^{25}$=−20.1 (*c* 0.97, $CHCl_3$, >99% ee).

4.4.3. (2*R*,3*S*)-3-Phenethyloxirane-2-carboxlic acid allylamide (21c). Colorless oil; IR (KBr) ν 3298, 3027, 2925, 1666, 1538, 1454, 1261, 905, 700 cm^{-1}; ^1H NMR ($CDCl_3$) δ 1.83–1.90 (m, 1H), 1.98–2.06 (m, 1H), 2.73–2.83 (m, 2H), 2.97–3.01 (m, 1H), 3.27 (d, J=2.0 Hz, 1H), 3.78–3.91 (m, 2H), 5.11–5.18 (m, 2H), 5.78 (ddd, J=17.0, 10.0, 5.5 Hz, 1H), 6.21 (br-s, 1H), 7.17–7.23 (m, 3H), 7.30 (d, J=7.5 Hz, 2H); ^{13}C NMR ($CDCl_3$) δ 31.8, 33.3, 41.0, 55.4, 59.0, 116.6, 126.2, 128.2 (×2), 128.5 (×2), 133.5, 140.4, 168.1; ESI-MS m/z 254 ($M+Na^+$). HRMS calcd for $C_{14}H_{17}NO_2$ (M^+): 231.1259. Found 231.1262. The enantiomeric excess was determined by chiral stationary-phase HPLC analysis (DAICEL CHIRALPAK AS-H, *i*-PrOH/hexane 1:4, flow rate 0.8 mL/min, t_R 16.2 min (minor isomer) and 26.4 min (major isomer), detection at 254 nm); $[\alpha]_D^{26}$=−4.05 (*c* 4.2, $CHCl_3$, 98% ee).

4.4.4. (2*R*,3*S*)-3-Phenethyloxirane-2-carboxlic acid cyclohexylamide (21d). White solid; IR (KBr) ν 3295, 3063, 3027, 2930, 2850, 1653, 1540, 1497, 1450, 1314, 1123, 1105, 899, 739, 695 cm^{-1}; ^1H NMR ($CDCl_3$) δ 1.07–1.19 (m, 3H), 1.31–1.38 (m, 2H), 1.58–1.72 (m, 2H), 1.79–1.91 (m, 2H), 1.98–2.04 (m, 1H), 2.73–2.83 (m, 2H), 2.94 (ddd, J=6.5, 4.6, 2.2 Hz, 1H), 3.23 (d, J=2.2 Hz, 1H), 3.69–3.76 (m, 1H), 5.95 (d, J=7.0 Hz, 1H), 7.18–7.31 (m, 5H); ^{13}C NMR ($CDCl_3$) δ 24.7 (×2) 25.4, 31.8, 32.9, 33.0, 33.4, 47.6, 55.5, 59.1, 126.2, 128.3 (×2) 128.5 (×2) 140.5, 167.4; ESI-MS m/z 296 ($M+Na^+$). HRMS calcd for $C_{17}H_{23}NO_2$ (M^+): 273.1729. Found 273.1723. The enantiomeric excess was determined by chiral stationary-phase HPLC analysis (DAICEL CHIRALPAK AS-H, *i*-PrOH/hexane 1:4, flow rate 0.5 mL/min, t_R 24.1 min (minor isomer) and 48.2 min (major isomer), detection at 254 nm); $[\alpha]_D^{28}$=+0.77 (*c* 0.78, $CHCl_3$, >99% ee).

4.4.5. (2*R*,3*S*)-3-Phenethyloxirane-2-carboxlic acid *tert*-butylamide (21e). Colorless oil; IR (neat) ν 3312, 3063, 3026, 2968, 1667, 1537, 1496, 1479, 1455, 1364, 1223, 896, 750, 700 cm^{-1}; ^1H NMR ($CDCl_3$) δ 1.33 (s, 9H), 1.81–1.89 (m, 1H), 1.99–2.06 (m, 1H), 2.73–2.84 (m, 2H), 2.93 (ddd, J=6.5, 4.6, 2.2 Hz, 1H), 3.14 (d, J=2.2 Hz, 1H), 5.88 (s, 1H), 7.19–7.31 (m, 5H); ^{13}C NMR ($CDCl_3$) d 28.6 (×2) 31.9, 33.4, 50.9, 55.8, 59.1, 126.2, 128.3 (×2), 128.6 (×2), 140.6, 167.5; ESI-MS m/z 270 ($M+Na^+$). HRMS calcd for $C_{15}H_{21}NO_2$ (M^+): 247.1572. Found 247.1576. The enantiomeric excess was determined by chiral stationary-phase HPLC analysis (DAICEL CHIRALPAK AS-H, *i*-PrOH/hexane 1:4, flow rate 0.5 mL/min, t_R 9.5 min (minor isomer) and 13.7 min (major isomer), detection at 254 nm); $[\alpha]_D^{25}$=+6.8 (*c* 0.78, $CHCl_3$, 99% ee).

4.4.6. (2*R*,3*S*)-3-Phenethyloxirane-2-carboxlic acid dimethylamide (21f). Colorless oil; IR (neat) ν 3480, 3025, 2930, 1652, 1496, 1455, 1398, 1264, 1154, 752, 701 cm^{-1}; ^1H NMR ($CDCl_3$) δ 1.98 (ddd, J=7.9, 7.0, 5.8 Hz, 2H), 2.76 (dt, J=14.0, 7.9 Hz, 1H), 2.86 (dt, J=14.0, 7.0 Hz, 1H), 2.94 (s, 3H), 2.97 (s, 3H), 3.19 (dt, J=2.1, 5.8 Hz, 1H), 3.32 (d, J=2.1 Hz, 1H), 7.18–7.30 (m, 5H); ^{13}C NMR ($CDCl_3$) δ 31.9, 33.3, 35.7, 36.2, 53.8, 57.5, 126.2, 128.4 (×2), 128.5 (×2), 140.8, 167.2; ESI-MS m/z 242 ($M+Na^+$). HRMS calcd for $C_{13}H_{17}NO_2$ (M^+): 219.1259. Found 219.1257. The enantiomeric excess was determined by chiral stationary-phase HPLC analysis (DAICEL CHIRALPAK AS-H, *i*-PrOH/hexane 1:4, flow rate 0.5 mL/min, t_R 42.8 min ((*2S,3R*)-isomer) and 51.8 min ((*2R,3S*)-isomer), detection at 254 nm); $[\alpha]_D^{26}$=−25.8 (*c* 0.97, $CHCl_3$, 99% ee).

4.4.7. (2*R*,3*S*)-(3-Phenethyloxiranyl)-pyrrolidin-1-yl-methanone (21g). Colorless oil; IR (neat) ν 3481, 2972, 2875, 1650, 1455, 1415, 1341, 910, 751, 701 cm^{-1}; ^1H NMR ($CDCl_3$) δ 1.78–2.05 (m, 6H), 2.75 (ddd, J=14.1, 8.3, 7.9 Hz, 1H), 2.87 (ddd, J=14.1, 8.2, 5.8 Hz, 1H), 3.16–3.21 (m, 1H), 3.18 (d, J=2.1 Hz, 1H), 3.23 (dt, J=2.1, 5.7 Hz, 1H), 3.43–3.52 (m, 3H), 7.18–7.30 (m, 5H); ^{13}C NMR ($CDCl_3$) δ 23.8, 26.1, 32.0, 33.2,?45.6, 46.2, 54.1, 57.4, 126.1, 128.4 (×2), 128.5 (×2), 140.8, 165.8; ESI-MS m/z 268 ($M+Na^+$). HRMS calcd for $C_{15}H_{19}NO_2$ (M^+): 245.1416. Found 245.1415. The enantiomeric excess was determined by chiral stationary-phase HPLC analysis (DAICEL CHIRALPAK AS-H, *i*-PrOH/hexane 1:1, flow rate 0.5 mL/min, t_R 30.9 min (minor isomer) and 43.5 min (major isomer), detection at 254 nm); $[\alpha]_D^{26}$=−32.1 (*c* 0.77, $CHCl_3$, >99% ee).

4.4.8. (2*R*,3*S*)-3-(4-Phenylbutyl)-oxirane-2-carboxlic acid methylamide (21h). White solid; IR (neat) ν 3277, 3107, 3026, 2936, 2853, 1662, 1567, 1451, 1412, 1268, 1162, 893, 749, 697 cm^{-1}; ^1H NMR ($CDCl_3$) δ 1.48–1.74

(m, 6H), 2.62 (t, J=7.3 Hz, 2H), 2.79 (d, J=5.2 Hz, 3H), 2.92 (dt, J=6.0, 2.1 Hz, 1H), 3.22 (d, J=2.1 Hz, 1H), 6.11 (br-s, 1H), 7.15–7.18 (m, 3H), 7.23–7.29 (m, 2H); ^{13}C NMR ($CDCl_3$) δ 25.2, 25.4, 31.0, 31.6, 35.7, 55.4, 59.6, 125.8, 128.3 (×2), 128.4 (×2), 142.1, 169.2; ESI-MS m/z 256 ($M+Na^+$). HRMS calcd for $C_{14}H_{19}NO_2$ (M^+): 233.1416. Found 233.1415. The enantiomeric excess was determined by chiral stationary-phase HPLC analysis (DAICEL CHIRALPAK AS-H, i-PrOH/hexane 1:4, flow rate 1.0 mL/min, t_R 13.5 min (minor isomer) and 24.7 min (major isomer), detection at 254 nm); $[\alpha]_D^{25}$=+21.8 (c 1.29, $CHCl_3$, >99% ee).

4.4.9. (2*R*,3*S*)-3-Propyloxirane-2-carboxlic acid benzylamide (22i). White solid; IR (KBr) ν 3223, 3065, 2954, 1654, 1560, 1451, 1257, 1030, 907, 696 cm^{-1}; ^{1}H NMR ($CDCl_3$) δ 0.97 (t, J=7.1 Hz, 3H), 1.47–1.66 (m, 4H), 2.95 (m, 1H), 3.27 (d, J=2.1 Hz, 1H), 4.42 (d, J=6.1 Hz, 2H), 5.80 (s, 1H), 7.26–7.35 (m, 5H); ^{13}C NMR ($CDCl_3$) δ 13.7, 19.0, 33.7, 42.8, 55.4, 59.6, 127.6, 127.7 (×2), 128.8 (×2), 137.6, 168.5; ESI-MS m/z 242 ($M+Na^+$). HRMS calcd for $C_{13}H_{17}NO_2$ (M^+): 219.1259. Found 219.1264. The enantiomeric excess was determined by chiral stationary-phase HPLC analysis (DAICEL CHIRALPAK AS-H, i-PrOH/hexane 1:4, flow rate 0.5 mL/min, t_R 26.3 min (minor isomer) and 41.5 min (major isomer), detection at 254 nm); $[\alpha]_D^{22}$=−1.78 (c 0.56, $CHCl_3$, 94% ee).

4.4.10. (2*R*,3*S*)-3-Cyclohexyloxirane-2-carboxlic acid benzylamide (20j).[28] The enantiomeric excess was determined by chiral stationary-phase HPLC analysis (DAICEL CHIRALPAK AS-H, i-PrOH/hexane 1:4, flow rate 0.5 mL/min, t_R 27.6 min ((2*R*,3*S*)-isomer) and 68.0 min ((2*S*,3*R*)-isomer), detection at 254 nm); $[\alpha]_D^{27}$=−4.14 (c 0.29, $CHCl_3$, >99% ee).

4.5. General procedure for the catalytic asymmetric epoxidation of β-aryl type α,β-unsaturated amides (condition B)

A THF solution (2.5 mL) of (*S*)-BINOL (7.2 mg, 0.025 mmol) and triphenylarsine oxide (8.1 mg, 0.025 mmol) was added to a stirred dry MS 4A (250 mg, dried for 3 h at 180°C under reduced pressure), then Sm(O-i-Pr)$_3$ (0.25 mL, 0.025 mmol, 0.1 M solution in THF) was added to the reaction mixture at room temperature. After stirring for 45 min at the same temperature, TBHP (0.077 mL, 0.6 mmol, 3.9 M solution in toluene) was added. After stirring for 10 min, **20k** (40.3 mg, 0.25 mmol) was added directly and the mixture was stirred at room temperature. After complete consumption of the starting material (18 h), the reaction mixture was diluted with ethyl acetate (10 mL) and quenched with 2% citric acid (2.5 mL). The water layer was extracted with ethyl acetate (10 mL), and the combined organic layers were washed with brine (5 mL) and dried over Na_2SO_4. After concentration in vacuo, the residue was purified by flash chromatography (SiO_2, hexane/ethyl acetate=4:1–3:1) to give epoxy amide **21k** (42.3 mg, 95%) as a white yellow solid.

4.5.1. (2*R*,3*S*)-3-Phenyloxirane-2-carboxlic acid methylamide (21k).[29] White yellow solid. The enantiomeric excess was determined by chiral stationary-phase HPLC analysis (DAICEL CHIRALPAK AS-H, i-PrOH/hexane 1:4, flow rate 1.0 mL/min, t_R 17.4 min ((2*S*,3*R*)-isomer) and 31.1 min ((2*R*,3*S*)-isomer), detection at 254 nm); $[\alpha]_D^{26}$=−50.8 (c 0.76, $CHCl_3$, >99% ee).

4.5.2. (2*R*,3*S*)-3-Phenyloxirane-2-carboxlic acid benzylamide (21l).[9] The enantiomeric excess was determined by chiral stationary-phase HPLC analysis (DAICEL CHIRALPAK AS-H, i-PrOH/hexane 1:4, flow rate 1.0 mL/min, t_R 25.0 min ((2*S*,3*R*)-isomer) and 62.2 min ((2*R*,3*S*)-isomer), detection at 254 nm); $[\alpha]_D^{25}$=−86.1 (c 0.62, $CHCl_3$, >99% ee).

4.5.3. (2*R*,3*S*)-3-Phenyloxirane-2-carboxlic acid dimethylamide (21m).[30] The enantiomeric excess was determined by chiral stationary-phase HPLC analysis (DAICEL CHIRALPAK AS-H, i-PrOH/hexane 1:1, flow rate 0.5 mL/min, t_R 23.3 min (minor isomer) and 28.5 min (major isomer), detection at 254 nm); $[\alpha]_D^{26}$=−109.4 (c 1.09, $CHCl_3$, >99% ee).

4.5.4. (2*R*,3*S*)-3-(4-Flurophenyl)-oxirane-2-carboxlic acid methylamide (21n). White solid; IR (KBr) ν 3300, 3121, 1652, 1578, 1509, 1413, 1219, 1155, 887, 841, 554, 528 cm^{-1}; ^{1}H NMR ($CDCl_3$) δ 2.87 (d, J=5.2 Hz, 3H), 3.50 (d, J=2.1 Hz, 1H), 3.86 (d, J=2.1 Hz, 1H), 6.25 (br-s, 1H), 7.04–7.07 (m, 2H), 7.23–7.27 (m, 2H); ^{13}C NMR ($CDCl_3$) δ 25.6, 58.5, 58.9, 115.7 (d, J=21.6 Hz) (×2), 127.5 (d, J=9.3 Hz) (×2), 130.72 (d, J=3.1 Hz), 163.1 (d, J=248 Hz), 167.8; ESI-MS m/z 218 ($M+Na^+$). HRMS calcd for $C_{10}H_{10}FNO_2$ (M^+): 195.0696. Found 195.0704. The enantiomeric excess was determined by chiral stationary-phase HPLC analysis (DAICEL CHIRALPAK AS-H, i-PrOH/hexane 1:4, flow rate 1.0 mL/min, t_R 20.5 min (minor isomer) and 40.0 min (major isomer), detection at 254 nm); $[\alpha]_D^{26}$=+39.7 (c 0.64, $CHCl_3$, 99% ee).

4.5.5. (2*R*,3*S*)-3-*p*-Tolyloxirane-2-carboxlic acid methylamide (21o). White solid; ^{1}H NMR ($CDCl_3$) δ 2.34 (s, 3H), 2.85 (d, J=5.0 Hz, 3H), 3.52 (d, J=2.0 Hz, 1H), 3.83 (d, J=2.0 Hz, 1H), 6.34 (s, 1H), 7.12–7.16 (m, 4H); ^{13}C NMR ($CDCl_3$) δ 21.2, 25.5, 58.9, 59.1, 125.7 (×2), 129.2 (×2), 131.8, 138.9, 168.2; ESI-MS m/z 214 ($M+Na^+$). HRMS calcd for $C_{11}H_{13}NO_2$ (M^+): 191.0946. Found 191.0940. The enantiomeric excess of **3o** was determined by chiral stationary-phase HPLC analysis (DAICEL CHIRALPAK AS-H, i-PrOH/hexane 1:4, flow rate 1.0 mL/min, t_R 18.7 min (minor isomer) and 37.9 min (major isomer), detection at 254 nm); $[\alpha]_D^{27}$=−53.4 (c 1.31, $CHCl_3$, >99% ee).

4.5.6. The absolute configurations of 21. The absolute configurations of **21k**[29] and **21l**[9] were determined by comparing between measured and reported optical rotations. The absolute configurations of **21a**, **21b**, **21f**, and **21j** were determined by comparing the measured optical rotations with authentic samples.[31]

Acknowledgements

This work was supported by CREST, The Japan Science and Technology Corporation (JST), RFTF of Japan Society for

the Promotion of Science (JSPS), and fellowship from JSPS (to T. N.).

References

1. For recent reviews, see: (a) Porter, M. J.; Skidmore, J. *Chem. Commun.* **2000**, 1215. (b) Nemoto, T.; Ohshima, T.; Shibasaki, M. *J. Synth. Org. Chem. Jpn* **2002**, *60*, 94.
2. For recent examples, see: (a) Corey, E. J.; Zhang, F.-Y. *Org. Lett.* **1999**, *1*, 1287. (b) Carde, L.; Davies, H.; Geller, T. P.; Roberts, S. M. *Tetrahedron Lett.* **1999**, *40*, 5421. (c) Nemoto, T.; Ohshima, T.; Shibasaki, M. *Tetrahedron Lett.* **2000**, *41*, 9569.
3. Juliá, S.; Masana, J.; Vega, J. C. *Angew. Chem., Int. Ed. Engl.* **1980**, *19*, 929.
4. (a) Bougauchi, M.; Watanabe, S.; Arai, T.; Sasai, H.; Shibasaki, M. *J. Am. Chem. Soc.* **1997**, *119*, 2329. (b) Watanabe, S.; Kobayashi, Y.; Arai, T.; Sasai, H.; Bougauchi, M.; Shibasaki, M. *Tetrahedron Lett.* **1998**, *39*, 7353. (c) Watanabe, S.; Arai, T.; Sasai, H.; Bougauchi, M.; Shibasaki, M. *J. Org. Chem.* **1998**, *63*, 8090. (d) Nemoto, T.; Ohshima, T.; Yamaguchi, K.; Shibasaki, M. *J. Am. Chem. Soc.* **2001**, *123*, 2725.
5. (a) Daikai, K.; Kamaura, M.; Inanaga, J. *Tetrahedron Lett.* **1998**, *39*, 7321. (b) Daikai, K.; Hayano, T.; Kino, R.; Furuno, H.; Kagawa, T.; Inanaga, J. *Chirality* **2003**, *15*, 83.
6. Jacobsen, E. N.; Deng, L.; Furukawa, Y.; Martínez, L. E. *Tetrahedron* **1994**, *50*, 4323.
7. (a) Armstrong, A.; Hayter, B. R. *Chem. Commun.* **1998**, 621. (b) Wang, Z. X.; Miller, S. M.; Anderson, O. P.; Shi, Y. *J. Org. Chem.* **1999**, *64*, 6443. (c) Solladié-Cavallo, A.; Bouérat, L. *Org. Lett.* **2000**, *2*, 3531. (d) Wu, X.-Y.; She, X.; Shi, Y. *J. Am. Chem. Soc.* **2002**, *124*, 8792.
8. Weitz, E.; Scheffer, A. *Ber. Dtsch. Chem. Ges.* **1921**, *54*, 2327.
9. (a) Nemoto, T.; Ohshima, T.; Shibasaki, M. *J. Am. Chem. Soc.* **2001**, *123*, 9474. (b) Nemoto, T.; Tosaki, S.-y.; Ohshima, T.; Shibasaki, M. *Chirality* **2003**, *15*, 306.
10. (a) Nemoto, T.; Kakei, H.; Gnanadesikan, V.; Tosaki, S.-y.; Ohshima, T.; Shibasaki, M. *J. Am. Chem. Soc.* **2002**, *124*, 14544. (b) Tosaki, S.-y.; Nemoto, T.; Ohshima, T.; Shibasaki, M. *Org. Lett.* **2003**, *5*, 495.
11. For a review, see: Ager, D. J.; Prakash, I.; Schaad, D. R. *Aldrichchim. Acta* **1997**, *30*, 3.
12. AM1 calculations were performed with the MOPAC version 6.
13. Frisch, M. J.; Trucks, G. W.; Schlegel, H. B.; Scuseria, G. E.; Robb, M. A.; Cheeseman, J. R.; Zakrzewski, V. G.; Montgomery, J. A. Jr.; Stratmann, R. E.; Burant, J. C.; Dapprich, S.; Millam, J. M.; Daniels, A. D.; Kudin, K. N.; Strain, M. C.; Tomasi, J.; Farkas, O.; Barone, V.; Cossi, M.; Cammi, R.; Mennucci, B.; Pomelli, C.; Adamo, C.; Clifford, S.; Ochterski, J.; Petersson, G. A.; Ayala, P. Y.; Cui, Q.; Morokuma, K.; Malick, D. K.; Rabuck, A. D.; Raghavachari, K.; Foresman, J. B.; Cioslowski, J.; Ortiz, J. V.; Baboul, A. G.; Stefanov, B. B.; Liu, G.; Liashenko, A.; Piskorz, P.; Komaromi, I.; Gomperts, R.; Martin, R. L.; Fox, D. J.; Keith, T.; Al-Laham, M. A.; Peng, C. Y.; Nanayakkara, A.; Gonzalez, C.; Challacombe, M.; Gill, P. M. W.; Johnson, B.; Chen, W.; Wong, M. W.; Andres, J. L.; Gonzalez, C.; Head-Gordon, M.; Replogle, E. S.; Pople, J. A. Calculations were performed with the Gaussian 98 program package; Revision A.7, Gaussian, Inc., Pittsburgh PA, 1998.
14. (a) Becke, A. D. *J. Chem. Phys.* **1993**, *98*, 5648. (b) Lee, C.; Yang, W.; Parr, R. G. *Phys. Rev. B* **1988**, *37*, 785.
15. For an example, see: Page, P. C. B.; Gareh, M. T.; Porter, R. A. *Tetrahedron Lett.* **1993**, *34*, 5159, and references therein.
16. For recent examples, see: (a) Furutani, T.; Imashiro, R.; Hatsuda, M.; Seki, M. *J. Org. Chem.* **2002**, *67*, 4599. (b) Imashiro, R.; Kuroda, T. *J. Org. Chem.* **2003**, *68*, 974, and references therein.
17. Asymmetric synthesis of α,β-epoxy amides using a highly enantioselective Darzens reaction of a camphor-derived sulfonium amide was reported, see: Aggarwal, V. K.; Hynd, G.; Picoul, W.; Vasse, J.-L. *J. Am. Chem. Soc.* **2002**, *124*, 9964.
18. For recent examples of tandem catalytic processes, see: (a) Jeong, N.; Seo, S.-D.; Shin, J.-Y. *J. Am. Chem. Soc.* **2000**, *122*, 10220. (b) Yamasaki, S.; Kanai, M.; Shibasaki, M. *J. Am. Chem. Soc.* **2001**, *123*, 1256. (c) Evans, P. A.; Robinson, J. E. *J. Am. Chem. Soc.* **2001**, *123*, 4609. (d) Louie, J.; Bielawski, C. W.; Grubbs, R. H. *J. Am. Chem. Soc.* **2001**, *123*, 11312. (e) Choudary, B. M.; Chowdari, N. S.; Madhi, S.; Kantam, M. L. *Angew. Chem., Int. Ed.* **2001**, *40*, 4620. (f) Bandini, M.; Cozzi, P. G.; Giacomini, M.; Melchiorre, P.; Selva, S.; Umani-Ronchi, A. *J. Org. Chem.* **2002**, *67*, 3700. (g) Tian, J.; Yamagiwa, N.; Matsunaga, S.; Shibasaki, M. *Angew. Chem., Int. Ed.* **2002**, *41*, 3636.
19. Addition of $Ph_3As{=}O$ retarded the epoxide opening reaction.
20. Reagents for the first epoxidation successfully prevented the formation of by-products. For the details, see Ref. 9a.
21. (a) Grimmelikhuijzen, C. J. P.; Rinehart, K. L.; Jacob, E.; Graff, D.; Reinscheid, H.-P.; Staley, A. L. *Proc. Natl. Acad. Sci., USA* **1990**, *87*, 5410. (b) Ishida, K.; Okita, Y.; Matsuda, H.; Okino, T.; Murakami, M. *Tetrahedron* **1999**, *55*, 10971.
22. Speranza, G.; Morelli, C. F.; Manitto, P. *Synthesis* **2000**, 123.
23. Orita, A.; Nagano, Y.; Hirano, J.; Otera, J. *Synlett* **2001**, 637.
24. He, L.; Byun, H.-S.; Bittman, R. *Tetrahedron Lett.* **1998**, *39*, 2071.
25. Calis, I.; Kuruüzüm, A.; Demirezer, L. O.; Sticher, O.; Ganci, W. *J. Nat. Prod.* **1999**, *62*, 1101.
26. For the detailed data, see the Supporting Information of Ref. 9b.
27. Rychnovsky, S. D.; Griesgraber, G. *J. Org. Chem.* **1992**, *57*, 1559.
28. Behrens, C. H.; Sharpless, K. B. *J. Org. Chem.* **1985**, *50*, 5696.
29. Meth-Cohn, O.; Moore, C.; Taljaard, H. C. *J. Chem. Soc., Perkin Trans. 1* **1988**, 2663.
30. Kuwano, R.; Takahashi, M.; Ito, Y. *Tetrahedron Lett.* **1998**, *39*, 1017.
31. For the detailed data, see the Supporting Information of Ref. 10a.